

## Sorption of Chlorhexidine on Cellulose: Mechanism of Binding and Molecular Recognition

Richard S. Blackburn,<sup>\*,†</sup> Anna Harvey,<sup>†</sup> Lorna L. Kettle,<sup>‡</sup> Avinash P. Manian,<sup>§</sup>  
John D. Payne,<sup>||</sup> and Stephen J. Russell<sup>†</sup>

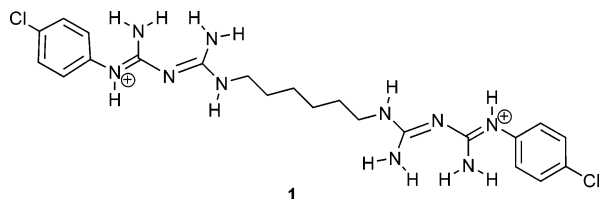
Green Chemistry Group, Centre for Technical Textiles, University of Leeds, Leeds, LS2 9JT, United Kingdom,  
Computational Chemistry Group, Intertek, Hexagon House, Blackley, Manchester, M9 8ZS, United Kingdom,  
Christian Doppler Laboratory for Textile and Fibre Chemistry in Cellulosics, Institute of Textile Chemistry and  
Textile Physics, University of Innsbruck, Höchsterstrasse 73, A-6850, Dornbirn, Austria, and Arch Chemicals  
(United Kingdom) Ltd., Hexagon House, Blackley, Manchester, M9 8ZS, United Kingdom

Received: January 31, 2007; In Final Form: May 24, 2007

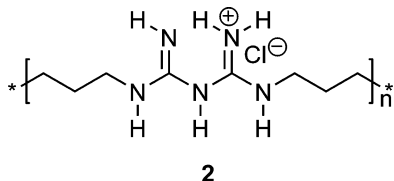
Chlorhexidine (CH) is an effective antimicrobial agent. There has been very little work published concerning the interactions of CH with, and its adsorption mechanism on, cellulose. In this paper, such physical chemistry parameters are examined and related to computational chemistry studies. Adsorption isotherms were constructed following application of CH to cellulose. These were typical of a Langmuir adsorption isotherm, but at higher concentrations displayed good correlation also with a Freundlich isotherm. Sorption was attributed to a combination of electrostatic (major contribution) and hydrogen bonding forces, which endorsed computational chemistry proposals: electrostatic interactions between CH and carboxylic acid groups in the cellulose dominate with a contribution to binding through hydrogen bonding of the biguanide residues and the *p*-chlorophenol moieties (Yoshida H-bonding) with the cellulose hydroxyl groups. At high CH concentrations, there is evidence of monolayer and bilayer aggregation. Differences in sorption between CH and another antimicrobial agent previously studied, poly(hexamethylenebiguanide) (PHMB), are attributed to higher molecular weight of PHMB and higher charge density of biguanide residues in CH (due to the relative electron withdrawing effect of the *p*-chlorophenol moiety).

## Introduction

Chlorhexidine (CH; **1**) is considered to be one of the most effective dental plaque inhibitors and the efficacy of CH against clinically significant microorganisms has been studied.<sup>1</sup> Anti-



microbial agents also find application in medical, apparel, and household textile sectors; one of the most important antimicrobial agents for textile applications, particularly cotton, is poly(hexamethylenebiguanide) (PHMB; **2**).<sup>2,3</sup> Previous work by the



authors has considered the sorption of PHMB onto cellulose.<sup>4</sup> Antimicrobial testing with *S. aureus* on CH-treated cotton

reveals that although there is some slight leaching from CH with a small zone of inhibition, antimicrobial activity is mainly an in situ process on the substrate (PHMB displays no zone of inhibition, hence no leaching<sup>2</sup>). There are many applications of CH as an effective antimicrobial agent; however, so far, it has not been reported to have been used commercially on textiles substrates, as a result there is little understanding of the interactions between CH and cellulose. In a study of adsorption of CH to contact lens hydrogels,<sup>1</sup> it was evident that CH has electrostatic interactions with negatively charged moieties of the hydrogel, its bonding strength dependent on charge density. The same study examined the adsorption of CH on sanitary cotton and suggested that an ion–ion interaction could occur between the protonated biguanide section of CH and anionic groups in the sanitary cotton.<sup>1</sup>

Understanding the mode of action fully, in particular the physical attractions that exist between the polymer and the substrate, could lead to developments in durability during washing, and to more efficient application processes by applying the optimum concentration of antimicrobial agent to achieve maximum binding strength with the substrate. Life cycle analysis work that has recently been carried out suggests that antimicrobial agents applied to cotton can potentially reduce the water, energy and chemical consumption in the life cycle of a treated product.<sup>5</sup> Furthermore, understanding the sorption mechanisms involved and molecular recognition for CH would allow future investigation of the application to other cellulosic fibers such as lyocell and viscose by understanding the groups in cellulosic fibers that are responsible for CH–fiber affinity. In the paper herein, such physical chemistry parameters are examined for

\* Corresponding author. E-mail: r.s.blackburn@leeds.ac.uk.

<sup>†</sup> University of Leeds.

<sup>‡</sup> Intertek.

<sup>§</sup> University of Innsbruck.

<sup>||</sup> Arch Chemicals Ltd.

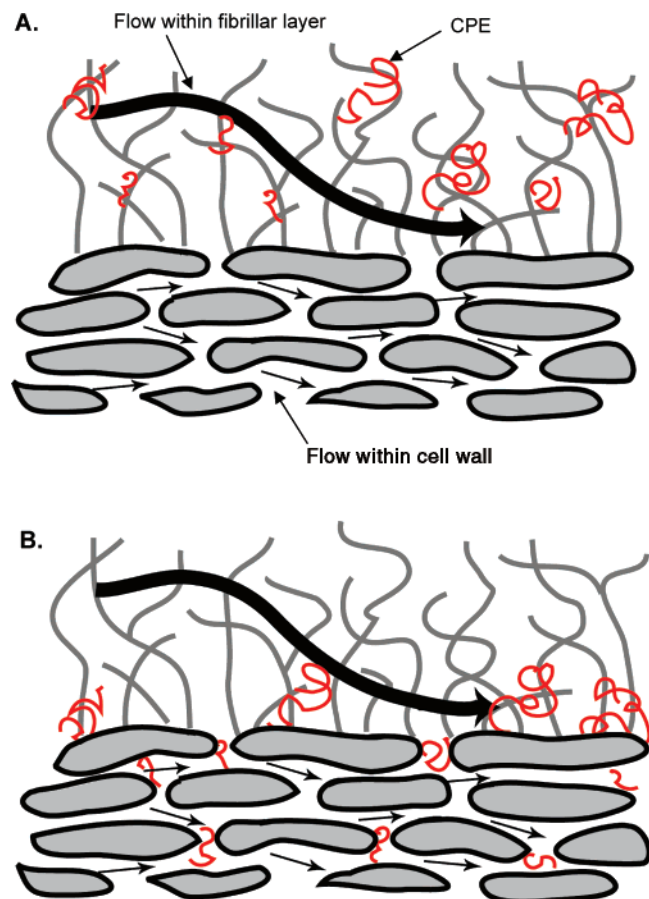


**Figure 1.** Continuous pore networks in cellulosic fibers. Liquid flow is shown within fibrillar layer at fiber–liquid interface and within the porous cell wall below. Part A: initial sorption of CPEs within pore structure of fibrillar layer. Part B: after passage of time, sorption of larger CPEs at surface of cell wall and sorption of smaller CPEs within cell wall pore structure.

CH through various experimental and analytical techniques and related to computational chemistry studies and sorption isotherm theory.

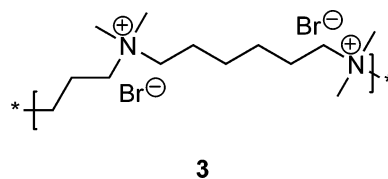
Cotton is mainly composed of cellulose, which is essentially a polymer of  $\alpha$ -D-glucose units in the  ${}^4C_1$  conformation with  $\beta$ -(1 $\rightarrow$ 4) linkages. Carboxylic acid (COOH) groups are formed in cellulose through oxidation of glucose rings during processing operations such as bleaching or mercerizing<sup>6</sup> and these provide anionic sites for adsorption.<sup>7</sup> Cellulosic fibers such as cotton have a complex structure comprising a system of fibrils and pores, shown schematically in Figure 1, which is a combination of proposals of the authors herein and other authors, particularly Hubbe.<sup>8</sup> At the fiber surface exists a layer of fibrils and microfibrils through which liquid can flow. It is probable that as the fibrils decrease in diameter their state in water changes from solid phase, through a gel phase, to a solution phase as fibrils can range all the way down to molecular dimensions;<sup>9</sup> this would make adsorption of sorbate molecules easier where sorption involves phase change from an aqueous phase to solid phase. Below the fibrillar layer exists a pore network within the cell wall, the main bulk of the fiber, through which liquid flow also occurs. In the fibrillar layer void spaces as large as 100  $\mu$ m may be expected,<sup>8</sup> which is up to 1000 times larger than the estimated sizes of the pores in the cell wall ranging from 10 to 300 Å in diameter,<sup>10,11</sup> with most pores in the range 50–100 Å;<sup>12</sup> hence, molecular mass is an important factor in adsorption. The thickness of the cell wall in cellulosic fibers is

approximately 10  $\mu$ m in the swollen state, which is a considerable distance, but evidence suggests that CPEs diffuse into the fiber from the surface as long as there is an electrostatic driving force for further adsorption.<sup>13</sup>

COOH groups exist within both the fibrillar layer and cell wall, providing anionic sites for adsorption. Adsorption of a cationic polyelectrolyte (CPE) on cellulose has been described in theory as an ion-exchange process with a close 1:1 stoichiometry between charges on polymer and charges on fiber; hence, one cationic center in the CPE associates with one carboxylic acid group in the cellulose.<sup>13–15</sup> Adsorption occurs by the following processes: transport of the CPE from solution to the fiber and adsorption of the CPE within the fibrillar layer at the surface of the cellulosic fiber (Figure 1A); reconfiguration of the CPE on the surface of the substrate; transportation of the CPE within the porous network of the fiber, relative to molecular size of the CPE (Figure 1B); detachment of the CPE from the surface (desorption).<sup>16</sup> The sorption system is in equilibrium when adsorption and desorption occur simultaneously. Figure 1B shows that smaller CPEs may be able to access the pore network of the cell wall, whereas larger CPEs may be excluded and restricted to sorption within the fibrillar layer at the fiber surface. Studies<sup>11,17,18</sup> have demonstrated that different CPEs reach different levels of the cell wall depending partly on their molecular mass, but mainly on their size (radius of gyration).

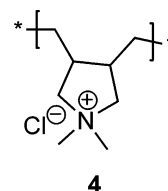
A detailed review of literature describing the sorption properties of high molecular weight CPEs on cellulose is given in previous work by the authors.<sup>4</sup> As CH has a molecular mass of 507 g mol<sup>-1</sup>, the literature reviewed here will focus on work with lower molecular weight CPEs.

Much work has been done by Wågberg on adsorption of CPEs on cellulose. Adsorption of low molecular mass 3,6-ionene (**3**;  $M_r$  6,000 g mol<sup>-1</sup>) in electrolyte concentrations less than 10<sup>-5</sup> M was rapid, and a 1:1 stoichiometry between the charges on the electrolyte and the carboxylic groups on the fiber was observed, indicating electrostatic attraction. For cellulose fibers



with varying carboxylic acid group content, the adsorption isotherm leveled with increasing application concentration, typical of a Langmuir isotherm. Maximum adsorption concentration up to 75 mg g<sup>-1</sup> for cellulose with carboxylic acid group content of 6.9% was observed.<sup>13</sup> Adsorption stoichiometry increased to 90% up to 20 mg g<sup>-1</sup> adsorbed, but then rapidly reduced to below 70% at higher application concentrations.<sup>14</sup>

In work examining the sorption of poly(diallyldimethylammonium chloride) (DADMAC) (**4**;  $M_r$  = 8750 g mol<sup>-1</sup>) on bleached cotton a Langmuir type adsorption isotherm was observed with a plateau region.<sup>12</sup> As the majority of pores in



cellulosic fibers have a range up to 50–100 Å, and it was proposed that the polymer needed to be smaller than 80 Å to

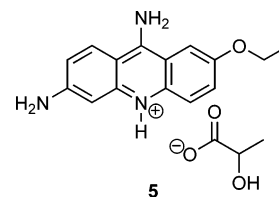
have accessibility to all charges in fiber wall. The radius of gyration ( $R_g$ ) of the low  $M_r$  DADMAC polymer was 86 Å and subsequently showed maximum adsorption at 11 mg g<sup>-1</sup> as it was able to reach all charges in fiber wall (high and medium  $M_r$  polymers displayed maximum adsorption at 2.5 mg g<sup>-1</sup> and were restricted to external surfaces of fibers). In terms of adsorption, it can be concluded that there exists a distinct relationship between the size of CPE molecules and the pore sizes of the fibrillar layer and the cell wall.

Initial work on the effect of salt concentration suggested that at low salt concentrations CPEs adsorb in a flat conformation and that adsorption increases with increasing salt concentration, however, work by van de Steeg et al. demonstrated that this is not the absolute case and considered the effects of screening.<sup>19</sup> In screening-enhanced adsorption, adsorption increases with increasing salt concentration because the salt screens repulsion between polymer segments and this is the dominating effect. In screening-reduced adsorption, adsorption decreases with increasing salt concentration because the dominating effect is the screening of attraction between CPEs and the substrate. If attraction is purely electrostatic, which operates over long ranges, the adsorption regime is always screening-reduced, over short ranges nonelectrostatic interactions exist and in this case both screening-enhanced and screening-reduced adsorption are found. For polyelectrolytes with a high charge density, the only driving force for adsorption is the charge interaction between polymer segments and the charge on the substrate. As salt concentration is increased, the interaction between the segments and the surface is decreased and the adsorption is hence decreased. When there is a nonelectrostatic contribution to adsorption, as electrolyte concentration is increased repulsion between polymer segments on the surface of the substrate is decreased and adsorption is increased. However, if there is a specific competition reaction between electrolyte counterions and the surface, then with increasing electrolyte concentration the adsorption will decrease. When polyelectrolytes have a low charge density adsorption always tends to be higher than for polymers with high charge density, but in general, adsorption decreases with increase in salt concentration, as adsorption relies upon both electrostatic and nonelectrostatic interactions.<sup>19</sup>

In addition to the adsorption of CPEs onto cellulose, work has been conducted concerning the adsorption of cationic surfactants. The general isotherm of surfactant adsorption onto oppositely charged surfaces describes three phases in the theoretical model: (1) ionic surfactant molecules are adsorbed individually through an ion-exchange mechanism with no interaction between adjacent surfactant molecules; (2) when the surfactants begin to interact, monolayered (hemimicelle) and bi-layered (admicelle) aggregates form which boost adsorption and gives a rise in adsorption; (3) the attractive interaction is counteracted by electrostatic repulsion of the charged head groups of the surfactants and the saturation plateau is attained.<sup>20–24</sup> Some authors describe two additional phases, where further hemimicelle and admicelle formation can allow a surface stacking effect.<sup>25,26</sup> Recent work by Alila et al. on the adsorption of cationic surfactants onto cellulose demonstrated that adsorption proceeded by electrostatic and dispersive interactions. Increase in the negative charge density of cellulose improved the electrostatic forces promoting surfactant adsorption and self-assembly, thus allowing dense packing of adsorbed molecules into hemimicelles and admicelles aggregates.<sup>27</sup>

The only previous study of the sorption of CH on cellulose focused on adsorption onto cotton for sanitary medical applica-

tions.<sup>1</sup> Adsorption at 20 °C followed a Langmuir isotherm, with maximum absorption of 4.06 mg g<sup>-1</sup>; sorption of the antimicrobial agent acrinol (**5**) gave maximum adsorption of 4.12 mg g<sup>-1</sup>. An equilibrium state was achieved faster in CH



than in acrinol; a little less than  $1 \times 10^{-5}$  M for the former and a little less than  $2 \times 10^{-5}$  M for the latter. This was attributed to a greater surface activity of CH than of acrinol. In the same study, Akaho and Fukumori also examined the sorption of CH onto carbon black and concluded that not only ion–ion interactions were involved in sorption, but also hydrophobic interactions between the chlorophenyl and hexane moieties of CH and the hydrophobic portion of carbon black.

In this paper, physical chemistry parameters that describe the adsorption of CH on cotton are examined through various experimental and analytical techniques and related to computational chemistry studies and sorption isotherm theory.

## Experimental Section

**Materials.** Chlorhexidine ( $M_r = 507.46$  g mol<sup>-1</sup>) was kindly supplied by Arch Chemicals in solid form. The fabric used was bleached, mercerized, 100% cotton, plain weave, 150 g m<sup>-2</sup>, supplied by Whaley's, Bradford, which had been washed five times using ECE detergent in a standard wash cycle. Eosin Y staining indicator (C.I. Acid Red 87; 2',4',5',7'-tetrabromofluorescein) and all other general chemicals were obtained from Aldrich.

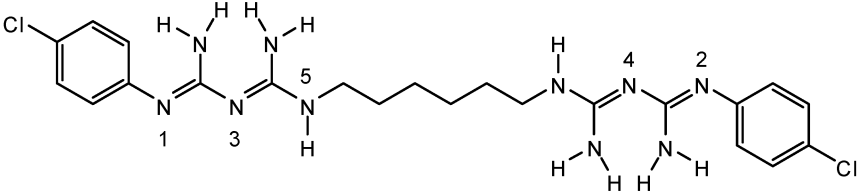
**Application of Chlorhexidine.** Cotton fabric (5 g) was immersed in an aqueous solution of CH, adjusted to pH 7 using 0.1% NaOH, then placed in stainless steel, sealed dye pots, housed in a laboratory-scale Roaches Pyrotec 2000 dyeing machine, using liquor: fiber ratio (LR) of 20:1. The pots were heated to 40 °C over 10 min and then held for 30 min at 40 °C, which is sufficient time for the sorption system to achieve equilibrium (application for extended periods did not result in higher or lower levels of adsorbate on substrate). After the application the liquor was retained and the pH measured (no deviation from initial pH was noted), and the fabric washed for 1 min under running cold tap water and dried at room temperature.

**UV/Visible Spectrophotometry.** The exhausted application baths were measured using a Jasco V-530 UV/Visible/NIR spectrophotometer at 219 nm, the wavelength of maximum absorption ( $\lambda_{\text{max}}$ ) for the residual CH solution. Concentrations were calculated from calibration graphs.

**Determination of Carboxylic Acid Group Content.** The COOH content was determined using the following literature method.<sup>28</sup> The dry weight of a sample (approximately 0.2 g) was recorded accurately and placed in a 100 cm<sup>3</sup> with 25 cm<sup>3</sup> of 0.03% methylene blue (C.I. Basic Blue 9) solution and 25 cm<sup>3</sup> of borate buffer solution (pH 8.5), and the bottle shaken at room temperature at speed 4 using a Heidolph Promax 2020 shaker for 20 h. Subsequently, 2.5 cm<sup>3</sup> of the residual solution and 5 cm<sup>3</sup> 0.1M HCl was diluted in a volumetric flask to 50 cm<sup>3</sup> with distilled water. Absorbance was measured using a Hitachi U-2000 spectrophotometer at the  $\lambda_{\text{max}}$  of the dye (664.5 nm) and concentrations were calculated from calibration



**TABLE 1: Ionization Sites and pK<sub>a</sub> Values of Chlorhexidine**

Structure and ionization sites	pK <sub>a</sub>		
	1	HL/H+L	10.15 ± 0.50
	2	H2L/H+HL	9.55 ± 0.50
	3	H3L/H+H2L	3.10 ± 0.70
	4	H4L/H+H3L	2.50 ± 0.70
	5	H5L/H+H4L	-4.46 ± 0.70

graphs. Each sample was repeated three times and an average COOH content calculated using eq 1, where *A* is total amount of free methylene blue (mg), and *E* is the weight of oven dry sample (g):

$$\text{mmol COOH g}^{-1} = \frac{0.00313(7.5 - A)}{E} \quad (1)$$

**Measurement of Zeta Potential.** Zeta potential ( $\zeta$ ) was determined using an Anton Paar Electrokinetic Analyzer (EKA) connected to an Anton Paar Remote Titration Unit (RTU), both units were operated using a PC and relevant software. Cotton was cut into 20 mm diameter disks using a metal die cutter; total mass was 1.0165 g. Fabric prior to the experiment was soaked in deionized water buffered with 0.1% NaOH to pH 7 for 6 h. Fabric discs were stacked one on top of another and carefully packed between the electrodes of the measurement cell. The distance between electrodes was maintained at 1.2 cm. The EKA machine was flushed with deionized water buffered at pH 7 with NaOH, a total volume of 600 cm<sup>3</sup> was held circulating the EKA. The RTU added 0.1 cm<sup>3</sup> of a 0.5% solution of chlorhexidine. The UV/spectrophotometry values of the start and after solutions were recorded. In concentrated systems, electrostatic interactions between solutes/particles must be accounted for. The resulting value of  $\zeta$  ( $\zeta_{\text{app}}$ ) is corrected ( $\zeta_{\text{corr}}$ ) for concentration as detailed in Delgado et al.<sup>29</sup>

### Computational Chemistry

The pK<sub>a</sub> values for the monomer units of CH were estimated using ACD Labs LogD software (V8) (Table 1); at pH 7, the ionized form is most likely the +2 form (H2L). The biguanide (BG) groups are in the same ionized form as predicted previously for PHMB (PHMB monomer has pK<sub>a</sub>s at approximately pK<sub>a1</sub> = 13.5 and pK<sub>a2</sub> = 3.03).<sup>4</sup> In comparison to PHMB, the first pK<sub>a</sub> for CH occurs at a lower pH indicating that it is easier to deprotonate, but harder to protonate, which is logical since although the *p*-chlorophenyl group is slightly electron donating, it has less electron donating character than an alkyl group (e.g., -C<sub>4</sub>H<sub>5</sub>) and therefore is comparatively electron withdrawing; withdrawing electron density from the BG group will make the adjacent N atom more difficult to protonate. The electron donating or withdrawing character can be estimated by the prediction of a selection of different Hammett substituent parameters (Table 2; negative values indicate substituents with electron donating character).

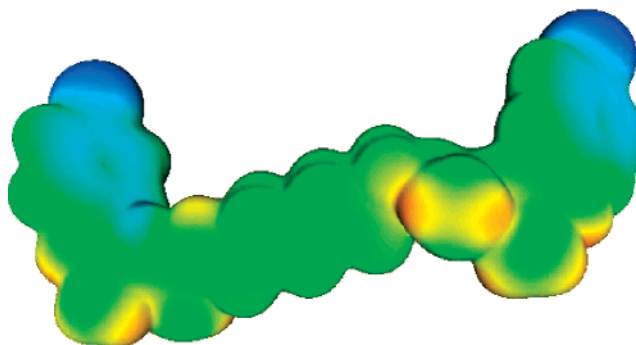
The geometry and the electronic properties of CH were explored using quantum mechanics methods (DFT/BPW91/6-31+G(d)) employing Gaussian 03 software and CHELPG

**TABLE 2: Hammett Substituent Parameters**

substituent	Hammett substituent parameter		
	$\sigma_p^+{}^a$	$\sigma_p^b$	$\sigma_{\text{ind}}^c$
CN	0.66	0.66	0.57
COOH	0.42	0.41	0.30
Cl	0.11	0.23	0.47
H	0	0	0
Ph	-0.18	0.01	0.12
Cl-Ph	-0.19	0.12	0.15
C <sub>4</sub> H <sub>5</sub>	-0.29	-0.16	-0.03
CH <sub>3</sub>	-0.31	-0.17	-0.01
NH <sub>2</sub>	-1.30	—	0.17

<sup>a</sup> Based on experimental data for substituents in the para position.

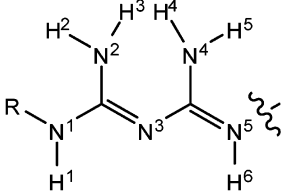
<sup>b</sup> For para substituents and an indication of their ability to stabilize a positive charge. <sup>c</sup> Represents the inductive component.



**Figure 2.** Electrostatic potential plotted onto a total electron density isosurface for CH (isocharge value of 0.002 atomic units (a.u.), which approximates the molecule's van der Waals radius and represents about 95% of the entire three-dimensional space occupied by the molecule). Blue is used to represent the strongest negative electrostatic potential on the molecule and red the strongest positive electrostatic potential. The other colors are the values in between, green is neutral.

(CHarges from ELectrostatic Potentials using a Grid based method<sup>30</sup>) charges calculated (Figure S.1). The electrostatic potential of CH was plotted on top of a total electron density isosurface (Figure 2). These computational models indicated that there was delocalization of the positive charge over each of the BG sections; the distribution is similar to that calculated for PHMB,<sup>4</sup> but the charge density ( $\alpha$ ) on each N and H atom studied for CH was higher in comparison with PHMB for each atom, respectively (Table 3). Greater electron withdrawing character of the *p*-chlorophenyl group in CH, compared with the -C<sub>4</sub>H<sub>5</sub> group used for PHMB, results in a higher  $\alpha$  of the atoms in biguanide group of CH.

**TABLE 3: CHELPG Charges on Biguanide Moiety of Chlorhexidine and PHMB**

General structure	Atom	CHELPG charges	
		CH (R = Ph-Cl)	PHMB (R = C <sub>4</sub> H <sub>9</sub> )
	N <sup>1</sup>	-0.763	-0.482
	N <sup>2</sup>	-1.071	-0.785
	N <sup>3</sup>	-0.859	-0.732
	N <sup>4</sup>	-0.929	-0.789
	N <sup>5</sup>	-0.584	-0.497
	H <sup>1</sup>	+0.406	+0.287
	H <sup>2</sup>	+0.475	+0.380
	H <sup>3</sup>	+0.455	+0.417
	H <sup>4</sup>	+0.428	+0.378
	H <sup>5</sup>	+0.432	+0.381
	H <sup>6</sup>	+0.345	+0.317

### Theoretical Basis

**Equilibrium Model.** In order to fully understand the sorption system involved between CH and cellulose, it is important to establish the most appropriate correlation for the equilibrium curves, which can be obtained by measuring the sorption isotherm of CH onto cellulose using experimental data.

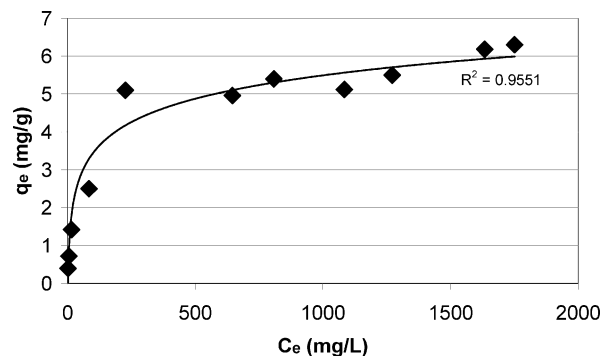
**Langmuir Isotherm.** The Langmuir isotherm describes sorption onto specific homogeneous sites within an adsorbent.<sup>31</sup> Langmuir's model of adsorption depends on the assumption that intermolecular forces decrease rapidly with distance and consequently predicts the existence of monolayer coverage of the adsorbate (CH) at the outer surface of the adsorbent (cellulose). It is then assumed that once a sorbate molecule occupies a site, no further adsorption can take place at that site. Moreover, the Langmuir equation is based on the assumption of a structurally homogeneous adsorbent where all sorption sites are identical and energetically equivalent and there is no interaction between molecules adsorbed on neighboring sites. Theoretically, the sorbent has a finite capacity for the sorbate. Therefore, a saturation value is reached beyond which no further sorption can take place. The saturated or monolayer (as  $C_1 \rightarrow \infty$ ) capacity can be represented by the expression represented in eq 2:

$$q_e = \frac{K_L C_e}{1 + a_L C_e} \quad (2)$$

where  $q_e$  is the equilibrium concentration of sorbate on the sorbent (solid-phase) (mg g<sup>-1</sup>),  $C_e$  is the equilibrium sorbate concentration in solution (mg dm<sup>-3</sup>), and  $K_L$  (dm<sup>3</sup> g<sup>-1</sup>) and  $a_L$  (dm<sup>3</sup> mg<sup>-1</sup>) are Langmuir constants. The constants  $K_L$  and  $a_L$  are evaluated through linearization of eq 2 (eq 3):

$$\frac{C_e}{q_e} = \frac{1}{K_L} + \frac{a_L}{K_L} C_e \quad (3)$$

Therefore, a plot of  $C_e/q_e$  versus  $C_e$  should yield a straight line of intercept value  $1/K_L$  and slope  $a_L/K_L$  if the isotherm obtained through experimental observes the Langmuir expres-

**Figure 3.** Adsorption isotherm of CH exhausted onto cellulose.

sion. The theoretical monolayer capacity is  $q_0$  and is numerically equal to  $K_L/a_L$ . However, the linearity of eq 2 is only respected at low solution concentrations, where the model follows Henry's law: as  $C_e$  becomes lower,  $a_L C_e$  is much less than unity and  $q_e = K_L C_e$ .

**Freundlich Isotherm.** The Freundlich isotherm<sup>32</sup> suggests that sorption energy exponentially decreases on completion of the sorptional centers of an adsorbent and describes heterogeneous systems, which are characterized by the heterogeneity factor  $1/n_F$ . When  $n = 1/n_F$ , the Freundlich equation reduces to Henry's law. Hence, the following empirical equation (eq 4) can be written:

$$q_e = K_F C_e^{1/n_F} \quad (4)$$

where  $q_e$  is the equilibrium concentration of sorbate on the sorbent (solid-phase) (mg g<sup>-1</sup>),  $C_e$  is the equilibrium sorbate concentration in solution (mg dm<sup>-3</sup>),  $K_F$  is the Freundlich constant (dm<sup>3</sup> g<sup>-1</sup>), and  $1/n_F$  is the heterogeneity factor. The capacity constant  $K_F$  and the affinity constant  $n_F$  are empirical constants dependent on several environmental factors. A linear form of the Freundlich isotherm can be obtained by taking logarithms of eq 4 (eq 5):

$$\ln q_e = \ln K_F + \frac{1}{n_F} \ln C_e \quad (5)$$

Therefore, a plot of  $\ln q_e$  versus  $\ln C_e$  should yield a straight line of intercept value  $\ln K_F$  and slope  $1/n_F$  if the isotherm obtained experimentally observes the Freundlich expression; if  $n > 1$ , then the adsorption is favorable. The Freundlich isotherm is another form of the Langmuir approach for adsorption on an "amorphous" surface where the amount of adsorbed material is the summation of adsorption on all sites. The Freundlich isotherm is derived by assuming an exponential decay energy distribution function inserted into the Langmuir equation. It describes reversible adsorption and is not restricted to the formation of the monolayer.

Thermodynamic data such as adsorption energy can be obtained from the Langmuir and Freundlich equations using eq 6, where  $K$  is constant in terms of dm<sup>3</sup> mol<sup>-1</sup>.<sup>33</sup>

$$-\Delta G^\circ = RT \ln K \quad (6)$$

### Results and Discussion

Results from UV/visible spectrophotometric analysis of residual CH solution in the exhausted application bath (Figure 3) demonstrated that as the concentration of active applied increases, the concentration of CH adsorbed also increases; the overall shape of this isotherm is typical of a Langmuir isotherm. Figures 4 and 5 show residual linear plots to demonstrate

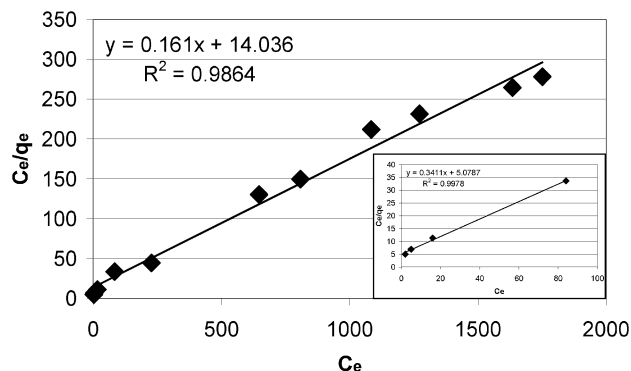


**Figure 4.** Plot of  $C_e/q_e$  vs  $C_e$  of data in adsorption isotherm of CH exhausted onto cellulose to  $C_0 = 2000 \text{ mg dm}^{-3}$ . Inset: plot of  $C_e/q_e$  vs  $C_e$  of data in adsorption isotherm of CH exhausted onto cellulose to  $C_0 = 200 \text{ mg dm}^{-3}$  only.

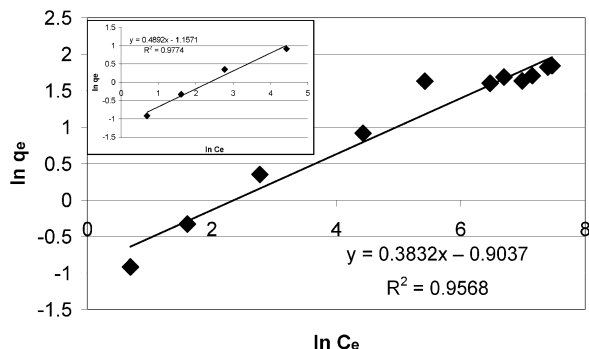


**Figure 5.** Log plot of data in adsorption isotherm of CH exhausted onto cellulose to  $C_0 = 2000 \text{ mg dm}^{-3}$ . Inset: log plot of data in adsorption isotherm of CH exhausted onto cellulose to  $C_0 = 200 \text{ mg dm}^{-3}$  only.

correlation ( $R^2$ ) to both Langmuir and Freundlich isotherms, respectively.

Table 4 shows a summary of the isotherm constants and correlation for both Freundlich and Langmuir isotherms in analysis of residual CH solution. It was observed that the isotherm correlation is closest to a Langmuir type, indicating limited site-specific adsorption (initial exponential rise and then plateau), as a result of electrostatic bonding forces between the delocalized positive charge in CH and carboxylate groups in cellulose.

However, good isotherm correlation is observed with respect to the Freundlich isotherm (logarithmic curve); adsorption by a Freundlich isotherm is indicative of unlimited adsorption of a species at nonspecific sites within a substrate, and in aqueous exhaustion of species onto cellulose is often an indication of adsorption via hydrogen bonding forces. Although the adsorption seems to be limited to the saturation value over the concentrations applied, it may be that there is also a contribution to affinity from hydrogen bonding.

In terms of the constants obtained from the plotted data, in the Freundlich expression if  $n_F > 1$ , then the adsorption is favorable, and this was observed. For the Langmuir expression, the theoretical monolayer capacity ( $q_0$ ) is numerically equal to  $K_L/a_L$ ; from the experimental data, it can be seen that the theoretical monolayer capacity of CH adsorption onto cellulose is  $7.0 \text{ mg g}^{-1}$  and is very close to the theoretical monolayer capacity of PHMB adsorption of  $5.3 \text{ mg g}^{-1}$  observed previously.<sup>4</sup>

Previous experimental studies have found that bleached, mercerized cotton fiber contains  $3 \times 10^{-5} \text{ mol}$  carboxylic acid groups per g fiber.<sup>34</sup> The results of the carboxylic acid group

content herein showed that the cotton used in the CH sorption studies had a COOH content of  $1.9 \times 10^{-5} \text{ mol g}^{-1}$ ; hence, if we consider CH ( $M_r = 578.4 \text{ g mol}^{-1}$ ), which has two cationic centers, binding through an electrostatic mechanism in 1:1 stoichiometry with two carboxylic acid groups, then the maximum mass of CH that can bind to the cotton used herein is  $5.49 \text{ mg g}^{-1}$ . The experimental value for the monolayer capacity of CH adsorption on cellulose observed herein at low concentrations (most reliable in Langmuir isotherms for monolayer calculations) of  $2.94 \text{ mg g}^{-1}$ , giving an adsorption stoichiometry of 53.6% for the monolayer; this value is not 100% of the sites available because of accessibility. The  $R_g$  of CH is approximately  $23 \text{ \AA}$  (as calculated and from literature<sup>1</sup>), and according to Stone et al.,<sup>35</sup> approximately 42% of a rayon fiber and 40% of cotton linters would be inaccessible to a polymer with molecular diameter of  $23 \text{ \AA}$ . It could be expected that bleached, mercerized cotton would display trends, in terms of the amorphous regions of the fiber, somewhere between rayon and cotton linters, hence, the adsorption stoichiometry of 53.6% is close to the 58–60% accessibility postulated, based on Stone et al. It is expected that CH would have the ability to diffuse into the cell wall of the fiber, which is in agreement with the work of Wågberg,<sup>12</sup> which demonstrated that a polymer needed an  $R_g$  below  $80 \text{ \AA}$  to reach all charges in the fiber cell wall.

It is expected that electrostatic forces would be the primary attractive force operating between cellulose and CH, in agreement with literature on adsorption of CPEs,<sup>13–15</sup> particularly at low application concentrations. Such electrostatic forces are stronger than hydrogen-bonding forces; this is evidenced by exhaustion figures of CH of over 80% at  $C_0 < 100 \text{ mg dm}^{-3}$ , which would be mainly through electrostatic attraction, although it is noted that these values are lower in comparison with the same range for PHMB where over 90% exhaustion was observed at  $C_0 < 100 \text{ mg dm}^{-3}$ . Sorption at higher concentrations, which also shows good correlation to a Freundlich isotherm (although higher  $R^2$  observed with Langmuir), suggests that interactions between the substrate and the adsorbate may occur by a combination of both electrostatic and hydrogen-bonding forces with the cellulose and potentially through interactions of CH with itself through some form of aggregation.

The main question that arises from a comparison of the sorption of CH and PHMB on cellulose (Table 4) is why PHMB displays significantly higher exhaustion. In terms of adsorption energy ( $\Delta G^\circ$ ), PHMB has a  $\Delta G^\circ$  of  $-20 \text{ kJ mol}^{-1}$ , whereas CH has a  $\Delta G^\circ$  of  $-12 \text{ kJ mol}^{-1}$ . The greater the chemical potential of the sorption system (more negative  $\Delta G^\circ$ ), the greater the sorption of sorbate onto sorbent; hence, values calculated from experimental data fitted to sorption isotherms reflect what is observed experimentally. The reasons for this observation must be related to two factors: the oligomeric nature, and hence higher molecular weight, of PHMB in comparison with CH (two biguanide units); and the electronic nature of the biguanide residues of each. The influence of these factors on interaction with cellulose and between separate sorbate molecules will determine sorption properties.

Previously calculated structural and electronic information was used to study molecular mechanical interactions. Simulations using molecular dynamics were used to explore the interaction of CH molecules with each other and with an idealized cellulose surface (for details see reference 4). Interactions between different functional groups in the solid state (Cambridge Crystallographic Structural Database) were mined to give information about preferred orientations and which atoms in the functional group dominate the different interactions. The

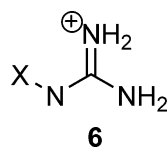
TABLE 4: Summary of the Isotherm Constants and the Correlation for Different Isotherms

sorbent (to $C_0 =$ )	Freundlich isotherm				Langmuir isotherm				
	$K_F$ ( $\text{dm}^3 \text{mol}^{-1}$ )	$n_F$	$R^2$	$\Delta G^\circ$ ( $\text{kJ mol}^{-1}$ )	$K_L$ ( $\text{dm}^3 \text{mol}^{-1}$ )	$a_L$ ( $\text{dm}^3 \text{mg}^{-1}$ )	$q_0$ ( $\text{mg g}^{-1}$ )	$R^2$	$\Delta G^\circ$ ( $\text{kJ mol}^{-1}$ )
CH <sup>a</sup> (200 $\text{mg dm}^{-3}$ )	160	2.04	0.977	−13.2	100	0.067	2.94	0.998	−12.0
CH <sup>a</sup> (5,000 $\text{mg dm}^{-3}$ )	206	2.61	0.957	−13.9	36	0.001	7.00	0.986	−9.3
PHMB <sup>b</sup> (500 $\text{mg dm}^{-3}$ )	2,852	2.46	0.906	−20.7	1,656	0.070	5.30	0.998	−19.3
PHMB <sup>b</sup> (5000 $\text{mg dm}^{-3}$ )	2,300	1.94	0.952	−20.1				0.670	

<sup>a</sup>  $M_r = 507.46 \text{ g mol}^{-1}$ , <sup>b</sup>  $M_r = 4600 \text{ g mol}^{-1}$ .

groups present in CH (e.g., the guanidino group, 4-chlorophenyl, Cl) were used as a central group to explore the interactions with the different functional groups present in the cellulose surface (Table 5).

The guanidino group (6) was used as a biguanide group was not available in the ISOSTAR software. Contour plots are useful



to examine the areas of high density of interactions: Only a small percentage of structures with both cellulose functional groups and an aromatic Cl have contacts within the van der Waals radii; interactions of the cellulose surface with the 4-chlorophenyl group are mainly with the phenyl hydrogen atoms. The percentage is much higher for the structures with both the guanidino group and the cellulose surface groups present, which may suggest that when CH interacts with a cellulose surface it is more likely to interact so via the BG group, although there may still be a significant contribution from the 4-chlorophenyl group.

The interaction of CH with an ideal cellulose surface was investigated using molecular mechanics methods (charges from DFT/BPW91/6-31G, Dreiding Forcefield). Interaction energies for a different combination of binding motifs were investigated (Table 6). Simulations were carried out using four CH molecules interacting with a cellulose surface (Figure S.2; each CH molecule was placed randomly above the cellulose surface); these were gas-phase MD calculations at 300 K (Cerius, charges from DFT/BPW91/6-31G, Dreiding Forcefield); binding motifs were noted and are summarized (Table S.1). Although there is significant evidence of electrostatic interaction between the cationic biguanide residues and the anionic carboxylic acid groups in the cellulose, hydrogen bonding between the biguanide residues and the cellulose hydroxyl groups is observed. However, the energy contribution from hydrogen bonding as a percentage of the total interaction energy is calculated at an average of 3.1%, against an average of 89.9% for the energy contribution from electrostatic interaction (the remainder being van der Waals energy). The contribution from hydrogen bonding for PHMB is significantly higher in comparison, and is a function of both  $M_r$  and the electronic structure of the biguanide residue.<sup>4</sup> There may also be some contribution due to the 4-chlorophenyl groups lying flat on the cellulose surface perhaps with some interactions between the phenyl hydrogens and the oxygens in the cellulose surface and interactions between the electron-deficient cellulose hydrogens and the  $\pi$ -electron system of the phenyl ring<sup>36</sup> through so-called Yoshida forces<sup>37</sup> (Figure 6).

Ionic strength is also a factor in adsorption;<sup>19,38</sup> in the initial application systems for CH used in this study, no electrolyte was added and the electrolyte concentration would be less than

$10^{-5} \text{ M}$ ,<sup>13</sup> and at such concentrations, adsorption would be at an optimum. Van de Steeg<sup>19</sup> noted that, as charge density of the polymer increases, there is a decrease in adsorption of the polyelectrolyte at low salt concentrations, as adsorption is not solely reliant upon electrostatic interactions and a significant contribution to adsorption arises from nonelectrostatic interactions. This may be one contributing factor in explaining the observation that PHMB has a significantly higher  $q_{e,\text{max}}$  than CH, which has the same biguanide moiety in its structure, but has a higher  $\alpha$  due to the relative electron withdrawing effect of the *p*-chlorophenol group.

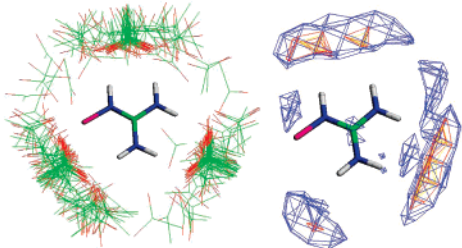
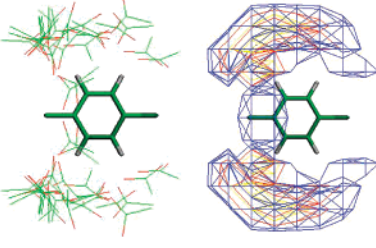
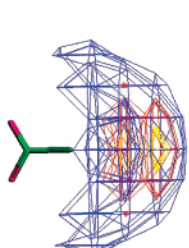
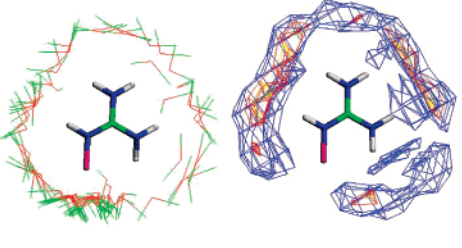
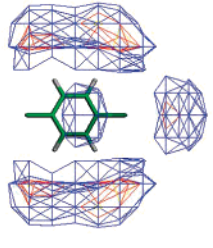
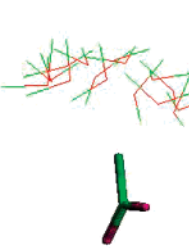
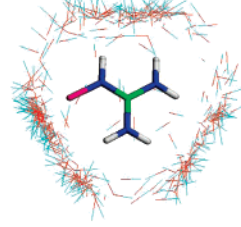
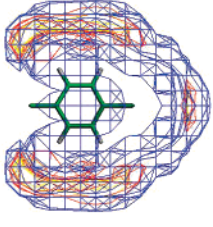
At all application concentrations of CH on cellulose, the pH of the system was pH 6–7. At this pH, the  $\zeta$  of raw cotton fibers is  $-10 \text{ mV}$ .<sup>39</sup> Pretreatment of cellulose fibers improves accessibility of dissociable groups; mercerization produces a pronounced increase in surface charge density and increases  $\zeta$  in the range pH 6–7 to  $-12 \text{ mV}$ .<sup>40</sup> By using streaming potential measurements,  $\zeta$  of bleached, and mercerized cotton in the range pH 6–7 has been determined to be  $-20$  to  $-25 \text{ mV}$ ,<sup>41,42</sup> which was in agreement with the results of EKA experiments conducted herein, giving an initial  $\zeta_{\text{corr}}$  of  $-24.5 \text{ mV}$ . Clearly, bleaching and mercerizing of cotton increases the electronegativity of the surface of the substrate and provides significant electrostatic potential for adsorption of CH.

Figure 7 shows the measurement values of  $\zeta$  plotted against the adsorption isotherm for CH on adsorption on cotton.  $\zeta_{\text{corr}}$  is initially negative and then increases rapidly until  $-9 \text{ mV}$  at approximately  $C_e = 20 \text{ mg dm}^{-3}$  and  $q_e = 1.5 \text{ mg g}^{-1}$ , from which point onward  $\zeta_{\text{corr}}$  remains constant, and  $q_e$  continues to increase significantly with increasing application concentration until  $5.0 \text{ mg g}^{-1}$ , thereafter increasing only slightly. This observation can be explained in terms of an initial neutralization of some of the negative charges in the fibrillar layer and the very periphery of the cell wall ( $\zeta_{\text{corr}}$  changes from  $-24.5 \text{ mV}$  to  $-9 \text{ mV}$ ) at low CH concentrations. As CH concentration increases  $\zeta_{\text{corr}}$  remains constant, but CH molecules continually diffuse within the cellulosic structure as the substrate presents a net negative charge at its surface. The strongly negative  $\zeta_{\text{corr}}$  with CH indicates that there is a strong diffusion of CH within the cellulosic fiber structure. The largely constant  $\zeta_{\text{app}}$  values in CH measurements, compared to the strong profile in the corresponding  $\zeta_{\text{corr}}$  values indicates that surface conductivity was significant in CH measurements, which essentially means that there is an accumulation of CH at the fiber/solution interface.<sup>29</sup> The interface is not limited only to the surface (fibrillar layer), but also occurs within the cell wall of the fiber, i.e., wherever the solution (CH + water) can gain access; this fact is a strong indicator of CH diffusion within the fiber.

Work by Alila et al.<sup>27</sup> on the adsorption of cationic surfactants onto cellulose demonstrated that adsorption proceeded by electrostatic and dispersive interactions allowing dense packing of adsorbed molecules into hemimicelles and admicelles aggregates, and this was manifest as an s-shaped isotherm for a plot of  $q_e$  versus  $\log C_e$ . While the experimental and compu-



**TABLE 5: ISOSTAR CSD Library of Functional Group Interactions for Chlorhexidine Functional Groups [Contour Plots Examine the Areas of High Density of Interactions (Yellow = High Density; Red = Medium Density; Blue = Low Density); for CSD Interacting Species, C is Green, O is Red, and H is Blue]**

Group in cellulose surface	Group in CH		
	Guanidino	4-chlorophenyl	Cl (Any aromatic – Cl in CSD)
COO <sup>−</sup>	$N_b^a = 69; N_c^b = 68; \%^c = 99$  <p>Interactions with COO<sup>−</sup> are more directional than with the aliphatic ether groups or hydroxyl groups</p>	$N_b = 32; N_c = 19; \% = 59$  <p>Mostly C–O...HpH interactions; <math>R = 2.41 \text{ \AA}</math></p>	$N_b = 941; N_c = 112; \% = 12$ 
Aliphatic ether	$N_b = 10; N_c = 8; \% = 80$ 	$N_b = 35; N_c = 11; \% = 31$  <p><math>R_2\text{--O...H--Ph}</math>; <math>R = 2.41 \text{ \AA}</math>; <math>R_2\text{--O...Cl}</math>; <math>R = 3.4 \text{ \AA}</math></p>	$N_b = 173; N_c = 8; \% = 5$  <p><math>R_2\text{--O...Cl}</math>; <math>R = 3.0\text{--}3.4 \text{ \AA}</math></p>
OH	$N_b = 157; N_c = 129; \% = 82$ 	$N_b = 147; N_c = 60; \% = 41$  <p>Some Cl...O–H interactions; <math>R = 3.2 \text{ \AA}</math></p> <p>Mainly HO...HpH interactions</p>	$N_b = 141; N_c = 8; \% = 6$ <p>Cl...O–H interactions; <math>R = 2.26 \text{ \AA}</math></p>

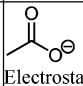
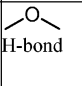
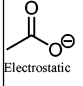
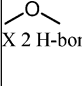
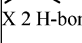
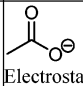
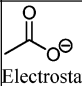
<sup>a</sup>  $N_b$  = number of crystal structures with the both groups present at contact distances. <sup>b</sup>  $N_c$  = number of crystal structures with the both groups present at contact distances with a distance ( $R$ ) less than the sum of van der Waals radii. <sup>c</sup>  $\% = 100.N_c/N_b$ .

tational work with CH does not describe classical micellar formation (although this would be worthy of further study), a residual plot after the work by Alila et al. does manifest a similar s-shaped isotherm as shown in Figure 7. In agreement with recent work of Alila et al.,<sup>43</sup>  $\zeta$  follows the same trend of the adsorption isotherm of CH on cellulose, and the abrupt increase in  $\zeta$  is associated with the onset of CH self-assembly and the

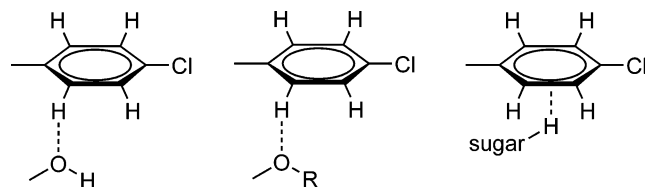
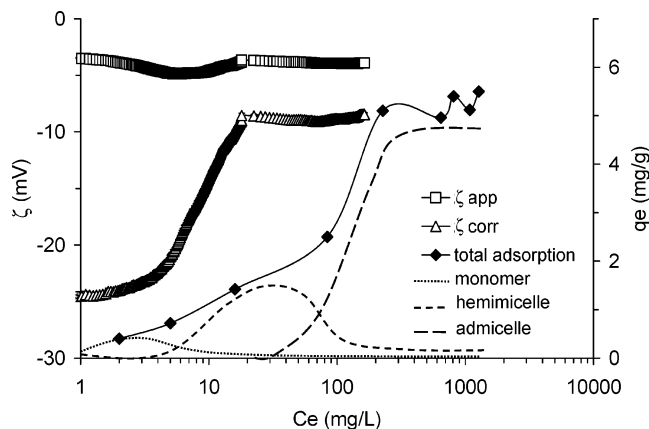
progressive neutralization of cellulose carboxylic moieties by the cationic centers of the CH molecule. The progressive formation of a plateau region is in agreement with the hypothesis of the generation of aggregates and saturation of the cellulosic substrate. Hemimicelle (monolayered aggregation) formation may be attributed to the side-to-side interactions of CH contributing to ordering on the surface, and admicelle (bilayered



**TABLE 6: Interaction Energies of Chlorhexidine with Groups in Cellulose**

	BG1	BG2	Energy contribution (kJ mol <sup>-1</sup> )	Total interaction energy (kJ mol <sup>-1</sup> )
1	 Electrostatic	 H-bond	$V^a = -55.48$ $E^b = -629.69$ $H^c = -21.17$	-706.26
2	 Electrostatic  H-bond	 X 2 H-bonds	$V = -46.02$ $E = -707.43$ $H = -26.19$	-782.03
3	 Electrostatic	 Electrostatic	$V = -7.196$ $E = -845.50$ $H = -24.76$	-877.55

<sup>a</sup> van der Waals energy. <sup>b</sup> Electrostatic energy. <sup>c</sup> Hydrogen-bonding energy.

**Figure 6.** Possible interactions of 4-chlorophenyl groups with cellulose.**Figure 7.** Plot of  $\zeta_{app}$  and  $\zeta_{corr}$  vs  $C_e$  and data in adsorption isotherm ( $q_e$  vs  $C_e$ ) of CH exhausted onto cellulose.

aggregation) formation attributed to various stacking interactions possible for CH. However, over the application concentration range used there does not appear to be any evidence of multilayer aggregation, which was observed for PHMB. This may be due to the smaller  $M_r$  of CH and the higher charge density, with respect to PHMB, which may reduce the propensity for hydrogen bonding.

## Conclusions

Adsorption isotherms were constructed by analysis of the residual baths following application of CH to cellulose. These were typical of a Langmuir adsorption isotherm, but at higher concentrations displayed good correlation also with a Freundlich isotherm. Sorption was attributed to a combination of electrostatic (major contribution) and hydrogen bonding forces, which

endorsed computational chemistry proposals: electrostatic interactions between CH and carboxylic acid groups in the cellulose dominate with a contribution to binding through hydrogen bonding of the biguanide residues and the *p*-chlorophenol moieties (Yoshida H-bonding) with the cellulose hydroxyl groups. At high CH concentrations, there is evidence from experimental data that monolayer aggregation (hemimicelle formation) and bilayer aggregation (admicelle) may contribute to increased adsorption and may explain the good correlation to the Freundlich isotherm. The differences between CH and PHMB sorption are attributed to the higher molecular weight of the PHMB and the higher charge density of the biguanide residues in CH because of the relative electron withdrawing effect of the *p*-chlorophenol moiety.

**Acknowledgment.** We would like to thank Arch Chemicals (U.K.) Ltd. and The Engineering and Physical Sciences Research Council for the provision of a Ph.D. CASE award scholarship to Miss Harvey. Thanks also to Yorkshire Forward Green Chemistry CIC for access to the Jasko V-530 UV–visible–NIR spectrophotometer and Christian Doppler Laboratory for Textile and Fibre Chemistry in Cellulosics for access to the Anton Paar Electrokinetic Analyser.

**Supporting Information Available:** Structure of CH with atoms labeled with CHELPG charges (Figure S.1), model of four CH molecules interacting with a cellulose surface (Figure S.2), and molecular dynamics simulations of interactions of CH with cellulose (Table S.1). This material is available free of charge via the Internet at <http://pubs.acs.org>.

## References and Notes

- Akaho, E.; Fukumori, Y. *J. Pharm. Sci.* **2001**, *90*, 1288.
- Payne, J. J. *Soc. Dyers Col.* **1997**, *113*, 48.
- Miller, W. M.; White, C. W. *Nonwovens World* **1986**, 129.
- Blackburn, R. S.; Harvey, A.; Kettle, L. L.; Payne, J. D.; Russell, S. J. *Langmuir* **2006**, *22*, 5636.
- Blackburn, R. S.; Payne, J. D. *Green Chem.* **2004**, *6* (7), G59.
- Nevell, T. P. In *The Dyeing of Cellulosic Fibres*; Preston, C., ed.; Dyers Co. Publications Trust: Bradford, U.K., 1986.
- Stana-Kleinschek, K.; Ribitsch, V.; Kreze, T.; Fras, L. *Mater. Res. Innovat.* **2002**, *6*, 13.
- Hubbe, M. A. *Bioresources* **2006**, *1* (1), 116.
- Pelton, R. *Nordic Pulp Paper Res. J.* **1993**, *8* (1), 113.
- Häggkvist, M.; Li, T.-Q.; Ödberg, L. *Cellulose* **1998**, *5*, 33.
- Alicie, B. J. *Appl. Polym. Sci.* **1990**, *39*, 355.
- Wågberg, L.; Häggkvist, R. *Langmuir* **2001**, *17*, 1096.
- Winter, L.; Wågberg, L.; Ödberg, L.; Lindström, T. *J. Colloid Interface Sci.* **1986**, *111* (2), 537.
- Wågberg, L.; Winter, L.; Ödberg, L.; Lindström, T. *Colloids Surf.* **1987**, *27*, 163.
- Wågberg, L.; Ödberg, L.; Lindström, T.; Aksberg, R. *J. Colloid Interface Sci.* **1988**, *123* (1), 287.
- van de Ven, T. G. M. *Adv. Colloid Interface Sci.* **1994**, *48*, 121.
- Lindström, T.; Söremark, K. *J. Colloid Interface Sci.* **1976**, *55*, 305.
- Tanaka, H.; Ödberg, L.; Wågberg, L.; Lindström, T. *J. Colloid Interface Sci.* **1990**, *134* (1), 229.
- van de Steeg, H. G. M.; Cohen Stuart, M. A.; de Keizer, A.; Bijsterbosch, B. H. *Langmuir* **1992**, *8*, 2538.
- Fuerstenau, D. W. *J. Colloid Interface Sci.* **2002**, *256*, 79.
- Koopal, L. K.; Lee, M. E.; Böhmer, M. R. *J. Colloid Interface Sci.* **1995**, *170*, 85.
- Harwell, J. H.; Hoskin, J.; Schechter, R. S.; Wade, W. H. *Langmuir* **1985**, *1*, 251.
- Adler, J. J.; Singh, P. K.; Patist, A.; Rabinovich, Y. I.; Shah, D. O.; Moudgil, B. M. *Langmuir* **2000**, *16*, 7255.
- Gouloub, T. P.; Koopal, L. K.; Bijsterbosch, B. H.; Sidorova, M. P. *Langmuir* **1996**, *12*, 3188.
- Łajtar, L.; Narkiewicz-Michalek, J.; Rudzinski, W. *Langmuir* **1994**, *10*, 3764.
- Li, B.; Ruckenstein, E. *Langmuir* **1996**, *12*, 5052.
- Alila, S.; Boufi, S.; Belgacem, M. N.; Beneventi, D. *Langmuir* **2005**, *21*, 8106.

- (28) Philipp, B.; Rehder, W.; Lang, H. *Papier* **1965**, 19, 1.
- (29) Delgado, A. V.; Gonzalez-Caballero, F.; Hunter, R. J.; Koopal, L. K.; Lyklema, J. *Pure Appl. Chem.* **2005**, 77 (10), 1753.
- (30) Breneman, C. M.; Wiberg, K. B. *J. Comput. Chem.* **1990**, 11, 361.
- (31) Langmuir, I. *J. Am. Chem. Soc.* **1916**, 38, 2221; Langmuir, I. *J. Am. Chem. Soc.* **1918**, 40, 1361.
- (32) Freundlich, H. M. F. *Z. Phys. Chem.* **1906**, 57, 385.
- (33) Kim, Y.; Kim, C.; Choi, I.; Rengraj, S.; Yi, J. *Environ. Sci. Technol.* **2004**, 38, 924.
- (34) Schleicher, H.; Lang, H. *Papier* **1994**, 48, 765.
- (35) Stone, J. E.; Treiber, E.; Abrahamson, B. *Tappi J.* **1969**, 52, 109.
- (36) Blackburn, R. S.; Burkinshaw, S. M. *J. Appl. Polym. Sci.* **2003**, 89, 1026.
- (37) Yoshida, Z.; Osawa, F.; Oda, R. *J. Phys. Chem.* **1964**, 68, 2895.
- (38) Ödberg, L.; Sandberg, S.; Welin-Klintström, S.; Arwin, H. *Langmuir* **1995**, 11, 2621.
- (39) Bellmann, C.; Caspari, A.; Albrecht, V.; Loan Doan, T. T.; Mäder, E.; Luxbacher, T.; Kohl, R. *Colloids Surf., A* **2005**, 267, 19.
- (40) Ribitsch, V.; Stana-Kleinschek, K.; Kreze, T.; Strnad, S. *Macromol. Mater. Eng.* **2001**, 286, 648.
- (41) Pušić, T.; Grancarić, A. M.; Soljačić, I.; Ribitsch, V. *J. Soc. Dyers Col.* **1999**, 115, 121.
- (42) Grancarić, A. M.; Tarbuk, A.; Pušić, T. *Color. Technol.* **2005**, 121, 221.
- (43) Alila, S.; Aloulou, F.; Beneventi, D.; Boufi, S. *Langmuir* **2007**, 23, 3723.